

ORIGINAL ARTICLE OPEN ACCESS

Sex Specific Effects of Environmental Toxin-Derived Alpha Synuclein on Enteric Neuronal-Epithelial Interactions

Hayley N. Templeton¹  | Alexis T. Ehrlich¹ | Luke A. Schwerdtfeger² | Julietta A. Sheng¹ | Ronald B. Tjalkens³ | Stuart A. Tobet^{1,4}

¹Department of Biomedical Sciences, Colorado State University, Fort Collins, Colorado, USA | ²Ann Romney Center for Neurological Disease, Harvard Medical School, Brigham and Women's Hospital, Boston, Massachusetts, USA | ³Department of Environmental and Radiological Health Sciences, Colorado State University, Fort Collins, Colorado, USA | ⁴School of Biomedical Engineering, Colorado State University, Fort Collins, Colorado, USA

Correspondence: Stuart A. Tobet (stuart.tobet@colostate.edu)

Received: 7 June 2024 | **Revised:** 4 February 2025 | **Accepted:** 31 March 2025

Funding: This study was supported by a National Institute of Mental Health (NIMH), "Sex Differences in Major Depression: Impact of Prenatal-Immune and Autonomic Dysregulation" (ORWH NIMH U54-MH118919) awarded to Multi-PIs, Goldstein/Tobet.

Keywords: alpha synuclein | calcitonin gene related peptide (CGRP) | goblet cells | Parkinson's disease | sex differences

ABSTRACT

Background: Parkinson's Disease (PD) is a neurodegenerative disorder with prodromal gastrointestinal (GI) issues often emerging decades before motor symptoms. Pathologically, PD can be driven by the accumulation of misfolded alpha synuclein (aSyn) protein in the brain and periphery, including the GI tract. Disease epidemiology differs by sex, with men twice as likely to develop PD. Women, however, experience faster disease progression, higher mortality, and more severe GI symptoms. Gut calcitonin gene-related peptide (CGRP) is a key regulator of intestinal contractions and visceral pain. The current study tests the hypothesis that sex differences in GI symptomatology in PD are the result of aSyn aggregation altering enteric CGRP signaling pathways.

Methods: To facilitate peripheral aSyn aggregation, the pesticide rotenone was administered intraperitoneally once daily for 2 weeks to male and female mice. Mice were sacrificed 2 weeks after the last rotenone injection, and immunohistochemistry was performed on sections of proximal colon.

Key Results: Levels of aSyn were heightened in PGP9.5 immunoreactive myenteric plexus neurons, a subset of which were immunoreactive to CGRP and showed a similar increase in aSyn immunoreactivity in rotenone-treated mice. Female mice exhibited 153% more myenteric aSyn, 26% more apical CGRP immunoreactivity in the mucosa, and 66.7% more aSyn in apical CGRP⁺ fibers after rotenone when compared to males. Goblet cell numbers were diminished, but the individual cells were larger in the apical regions of crypts in the colons of rotenone-treated mice with no difference between males and females.

Conclusions: This study used a mouse model of PD to uncover sex-specific alterations in enteric neuronal and epithelial populations, underscoring the importance of considering sex as a biological variable while investigating prodromal GI symptoms.

1 | Introduction

Parkinson's disease (PD) is a neurodegenerative disorder with gastrointestinal (GI) symptoms including bloating, visceral pain, gastroparesis, and constipation, seen in 10%–70% of PD subjects [1, 2] that can manifest up to 20 years before diagnosis [3]. GI symptoms impact quality of life and pose significant health risks

including malnutrition, intestinal obstruction, and impaired medication effectiveness [4, 5]. PD is driven pathologically by the accumulation of misfolded alpha synuclein (aSyn) protein in the brain and periphery, including the GI tract. Environmental toxins such as rotenone exacerbate aSyn aggregation, producing PD-like pathology and symptoms when administered to rodents [6]. Gut pathology in rotenone PD models includes peripheral

This is an open access article under the terms of the [Creative Commons Attribution-NonCommercial](https://creativecommons.org/licenses/by-nc/4.0/) License, which permits use, distribution and reproduction in any medium, provided the original work is properly cited and is not used for commercial purposes.

© 2025 The Author(s). *Neurogastroenterology & Motility* published by John Wiley & Sons Ltd.

Summary

- Mouse model of Parkinson's Disease (PD) was used to investigate sex-specific impact of enteric alpha synuclein (aSyn) on colonic goblet cells and CGRP⁺ neurons and fibers.
- Sex-specific alterations in intestinal neuronal and epithelial signaling pathways in response to aSyn provide insight into sex differences in PD etiology and prodromal gastrointestinal symptoms.

gastroparesis [7] and decreased intestinal transit [8, 9], creating a viable murine model for investigating mechanisms of GI dysfunction in PD.

Females with PD exhibit faster disease progression and higher mortality rates than males [10]. In addition, females with PD report more GI symptoms with higher severity [11–13], including constipation and abdominal pain, symptoms that heavily impact quality of life [14] and are among the earliest PD symptoms [15, 16]. Aggregation of aSyn in the intestinal wall alters gut immune populations [17], and sex differences in immune responses are abundant systemically [18], and peripherally in the gut mucosal immune system [19]. Roles of peripheral immune influence on enteric neurons and epithelial populations involved in prodromal PD gut symptomatology are not well elucidated.

Calcitonin gene related peptide (CGRP) is a neuropeptide implicated in the regulation of GI motility, inflammation, and nociception through dorsal root ganglia (DRG) afferents [20] and intrinsic enteric neurons [21, 22]. There are two forms of CGRP, α and β , which share around 90% homology [23] and have nearly identical biological activity [24, 25]. While not extensively characterized, there are likely classes of intrinsic sensory neurons (IPANs) in the myenteric plexus that express β CGRP [26, 27] and α CGRP [28]. Therapeutic interventions targeting α CGRP significantly inhibit colonic transit, leading to constipation [29, 30], while elevated α CGRP is associated with diarrhea, suggesting that α CGRP plays a role in GI motility [29]. Gut mucus regulates intestinal transit by acting as a lubricant to decrease physical resistance, and altered mucus levels influence GI transit time [31, 32]. CGRP produced by enteric neurons modulates goblet cell mucus secretion [33], as well as motility [34], further pointing towards CGRP involvement in intestinal transit regulation. Accumulation of aSyn in enteric neurons likely influences gut motility, driven by cholinergic neurons [35, 36]. However, the impact of aSyn accumulation in subsets of enteric cholinergic neurons, including CGRP⁺ cells, on mucosal neuroepithelial signaling remains to be seen. Determining if enteric CGRP⁺ neurons and mucosal projecting fibers accumulate aSyn in a mouse model of PD would provide valuable data towards understanding the altered GI function observed in PD.

To investigate the relationship of sex in aSyn accumulation in enteric CGRP fibers and provide a read out of goblet cell morphological alterations, a rotenone model of PD was utilized. Levels of aSyn were quantified in CGRP-expressing myenteric neurons and mucosal fibers. In addition, goblet cell anatomic localization and morphology were analyzed. Data from the present study

underscore the importance of examining sex-selective mechanisms in PD-related GI dysfunction, providing crucial insights into some of the earliest prodromal symptoms in PD.

2 | Materials and Methods

2.1 | Animals

Male and female C57BL/6J background mice aged 3–4 months were used for these studies. All animal protocols were approved by the Institutional Animal Care and Use Committee (IACUC) and Colorado State University Lab Animal Resources under protocol CoA # 1657. Mice were housed on a 12-h light/dark cycle with access to standard chow (Envigo TD.2918) and water *ad libitum*.

2.2 | Rotenone Preparation and Injections

Rotenone was prepared as a 50 \times stock dissolved in 100% dimethyl sulfoxide (DMSO) and stored in amber septa vials at -20°C . This solution was then diluted in medium-chain triglyceride, Miglyol 812N, to obtain a final concentration of 2.5 mg/mL rotenone in 98% Miglyol 812N, 2% DMSO. Rotenone was prepared fresh every other day. Mice were weighed every day and received intraperitoneal injections at a dose of 2 $\mu\text{L/g}$ body weight once daily for 14 days. The optimal dose was determined in a previous publication [37]. Fourteen days after the last rotenone injection, mice were deeply anesthetized with isoflurane and terminated via decapitation. The intestine was removed from the stomach to the colon and placed in 4% paraformaldehyde (PFA) at 4°C for 24 h. Tissue was subsequently placed in 1X phosphate buffered saline (PBS) at 4°C until sectioning.

2.3 | Immunohistochemistry

Fifty micrometre thick sections were prepared from 1 to 3 mm pieces of proximal colon and submerged in 4% agarose. The tissue was in agarose for a total of 9 min: 5 min on a room temperature shaker and 4 min at 4°C to ensure polymerization. Tissue was cut at a thickness of 50 μm on a vibrating microtome (VT1000S; Leica microsystems, Wetzlar, Germany). Sections were washed in 1 \times PBS for 10 min at 4°C and incubated in 0.1 M glycine for 30 min at 4°C , followed by three 5 min PBS washes. Next, tissue sections were incubated in 0.5% sodium borohydride at 4°C for 15 min, followed by three 5 min PBS washes. Sections were blocked in PBS with 5% normal goat serum (NGS; Lampire Biological, Pipersville, PA), 1% hydrogen peroxide, and 0.3% Triton X (Tx) for 1 h at 4°C with a change of solution at 30 min. Following blocking, sections were placed into primary antisera or lectin that is detailed in Table 1.

2.3.1 | Goblet Cell Lectin Histochemistry

The lectin *Ulex europaeus* Agglutinin I conjugated with Rhodamine (UEA-1; Vector Labs) was used at a concentration of 0.625 $\mu\text{g/mL}$ (Table 1) in PBS containing 5% NGS and 0.3% Tx for 2 days at 4°C . Sections were then washed four times at

TABLE 1 | Primary antibodies/lectin used.

Primary antibody/ lectin	Immunizing antigen	Raised	Dilution	Source	Catalog number
PGP9.5	Recombinant full length human UCHL1 purified from <i>E. coli</i>	Chicken	1:500	Novus Biologicals	NB110-58872SS
CGRP	Full length rat α -CGRP	Rabbit	0.625 μ g/mL	ImmunoStar	24,112
aSyn	Rabbit α -synuclein (D37A6)	Rabbit	1:500	Cell Signaling	4179
UEA-1, Rhodamine	N/A	N/A	0.625 μ g/mL	Vector Labs	RL-1062-2

TABLE 2 | Secondary antibodies used.

Secondary antibody	Conjugate	Dilution	Source	Catalog number
Goat anti-rabbit IgG	Alexa Fluor 405	1:500	Invitrogen	A-31556
Goat anti-chicken IgY	Alexa Fluor 568	1:500	Abcam	ab175477
Goat anti-rabbit IgG	Alexa Fluor 594	1:500	Invitrogen	A-11037
Goat anti-rabbit IgG	Alexa Fluor 647	1:500	Invitrogen	A-31573
Biotin-SP donkey anti-rabbit IGG	Biotin-SP	1:2500	Jackson ImmunoResearch	711,065,152

15 min intervals in PBS with 0.02% Tx, followed by four PBS washes. Finally, sections were mounted on slides and cover slipped with an aqueous mounting medium (Aqua-Poly/Mount, Polysciences, Warrington, PA).

2.3.2 | PGP9.5 and aSyn Immunohistochemistry

Sections were incubated for 2 days at 4°C in primary antisera containing anti-Protein Gene Product (PGP) 9.5 (Novus Biologicals, Centennial, CO) at 1:500 and anti-alpha-Synuclein (Cell Signaling, Danvers, MA) at 1:500 in PBS containing 5% NGS and 0.3% Tx. The aSyn antibody labels total aSyn per the vendor and several publications [38–40]. Following primary antisera incubation, sections were washed at room temperature in PBS with 1% NGS and 0.32% Tx four times at 15 min intervals. Sections were then incubated for 2 h in secondary antibodies to the appropriate species (Alexa Fluor 405 anti-rabbit and Alexa Fluor 568 anti-chicken; Table 2) at 1:500 constituted in PBS with 0.32% Tx. Following secondary antibody incubation, sections were washed four times at 15 min intervals in PBS with 0.02% Tx, followed by four PBS washes. Finally, sections were mounted on slides and cover slipped with an aqueous mounting medium (Aqua-Poly/Mount, Polysciences, Warrington, PA).

2.3.3 | CGRP and aSyn Immunohistochemistry

Sections were incubated for 2 days at 4°C in primary antisera containing anti-aSyn (Cell Signaling, Danvers, MA) at 1:500 in PBS containing 5% normal donkey serum (NDS) and 0.3% Tx. A negative control of the aSyn antibody revealed no signal (Figure S1C). Sections were then washed four times at 15 min intervals in PBS with 1% NDS and 0.32% Tx at room temperature. Next, sections were incubated for 2 h at room

temperature in biotinylated donkey-anti-rabbit (Table 2, Jackson ImmunoResearch Laboratories Inc., West Grove, PA) at 1:2500 constituted in PBS with 0.32% Tx. Sections were washed four times at 15 min intervals in PBS with 0.02% Tx at room temperature before incubation in Alexa Fluor 594-streptavidin (Invitrogen) at 1:500 for 1 h. Sections were then washed four times at 15 min intervals in PBS with 0.02% Tx at room temperature. Sections were incubated for 2 days at 4°C in primary antisera containing anti- α CGRP (ImmunoStar, Hudson, WI) at 0.625 μ g/mL in PBS containing 5% NGS and 0.3% Tx. Of note, this antibody likely labels a small percentage of β CGRP; however, signal was only partially extinguished in β CGRP pre-absorption studies performed by the vendor. A pre-absorption with full length α CGRP peptide (AnaSpec, Fremont, CA) eliminated signal (Figure S1A) and there was no signal in controls with secondary antisera omitted (Figure S1B). Following primary antibody incubation, sections were then washed four times at 15 min intervals in PBS with 0.02% Tx before incubation in Alexa Fluor 647 (Table 2, Invitrogen, Waltham, MA) at 1:500 for 2 h at room temperature. Sections were then washed four times at 15 min intervals in PBS with 0.02% Tx, followed by four PBS washes. Finally, sections were mounted on slides and cover slipped with an aqueous mounting medium (Aqua-Poly/Mount, Polysciences, Warrington, PA).

2.4 | Tissue Imaging & Analysis

Images were taken using a Zeiss LSM800 upright confocal laser scanning microscope and a 40 \times or 63 \times (EC Plan-Neofluar) oil immersion objective. High-resolution images were taken using a Zeiss LSM880 upright confocal microscope with an AxioCam 503 monochromatic camera and a 63 \times (Plan-Apochromat) oil immersion objective. Data for CGRP and aSyn and goblet cell analyses was gathered from

confocal Z-stacks with 15 planes 1 μm apart, with the top and bottom planes set from the focus of labeling. Z-stacks were acquired for all four sections per group, and three crypts per section were imaged. Max intensity Z-projections were performed, and regions of interest (ROIs) were defined as the apical or basal half of a crypt. Apical and basal regions were defined by measuring the length of a crypt and dividing it into two equal parts. ROIs were gathered from 12 crypts per animal and averaged. aSyn and PGP 9.5 analyses were gathered from individual, single-plane confocal images. Control areas for aSyn and PGP9.5 colocalization were initially defined as muscle regions with no PGP9.5-ir. These regions had no aSyn-ir. Twelve 50 μm \times 50 μm ROIs containing aSyn and PGP 9.5 double labeling were selected per sample. aSyn and CGRP analyses were gathered from 20 μm z-projection confocal images. The apical half of six crypts and six myenteric neurons containing aSyn and CGRP double labeling were selected per animal from 20 μm z-projection confocal and subsequently averaged. All image acquisition and analyses were performed by a researcher blinded to treatment. All image analyses were performed using Fiji (v1.0; NIH). Goblet cell quantity and size were measured using the analyze particles tool in Fiji. Images were thresholded based on optical density, and a binary watershed was applied prior to quantification. Mean goblet cell size was calculated based on the area as measured by analyze particles for individual anatomic ROIs as described above. The immunoreactive percentage of area labeled was calculated using the 'measure' tool in Fiji on thresholded images restricted to the defined ROI for each respective analysis. To determine the % area of aSyn in CGRP neurons/fibers, thresholded CGRP-IR images were used to generate ROIs using the analyze particles tool. Thresholded aSyn-IR images were then analyzed using CGRP ROIs as area restrictions. Then, the percentage of total CGRP-IR area that contained aSyn-IR was calculated.

2.5 | Statistics

All statistical analyses were performed using Graphpad Prism version 10.1.2 (Graphpad Software, La Jolla, CA). For aSyn and PGP 9.5 average area, CGRP area, and percent area of aSyn in CGRP, a two-way ANOVA was performed by treatment and sex. For goblet cell number and size, a three-way ANOVA was performed by treatment, region, and sex. All data are presented as means \pm standard error of the mean (SEM). In all instances where *p* values are noted, a post hoc Tukey's multiple comparison test was performed to compare individual means. A Brown-Forsythe equality of variance test was performed for all two-way ANOVAs to confirm variances were not significantly different across groups. For three-way ANOVAs, a Spearman's test for heteroscedasticity was used to confirm equal error.

3 | Results

3.1 | Rotenone Treatment Increased Myenteric Plexus aSyn

To verify that mice responded to rotenone treatment, body weight was measured daily throughout the entirety of the experiment. The experimental timeline is outlined in Figure 1A. Mice had similar starting body weights regardless of treatment group (vehicle: 24.2g \pm 5, rotenone: 21.8g \pm 0.8) (Figure 1B). Change in weight was measured by subtracting starting weight from each daily weight measurement. Rotenone treatment resulted in blunted weight gain in males (Figure 1C) and females (Figure 1D). As a further measurement of rotenone impact, a researcher blind to treatment correctly identified treatment groups based on a 5-min open field behavior test. Rotenone-treated mice exhibited decreased exploratory movement and alterations in gait, similar to our previous findings [37].

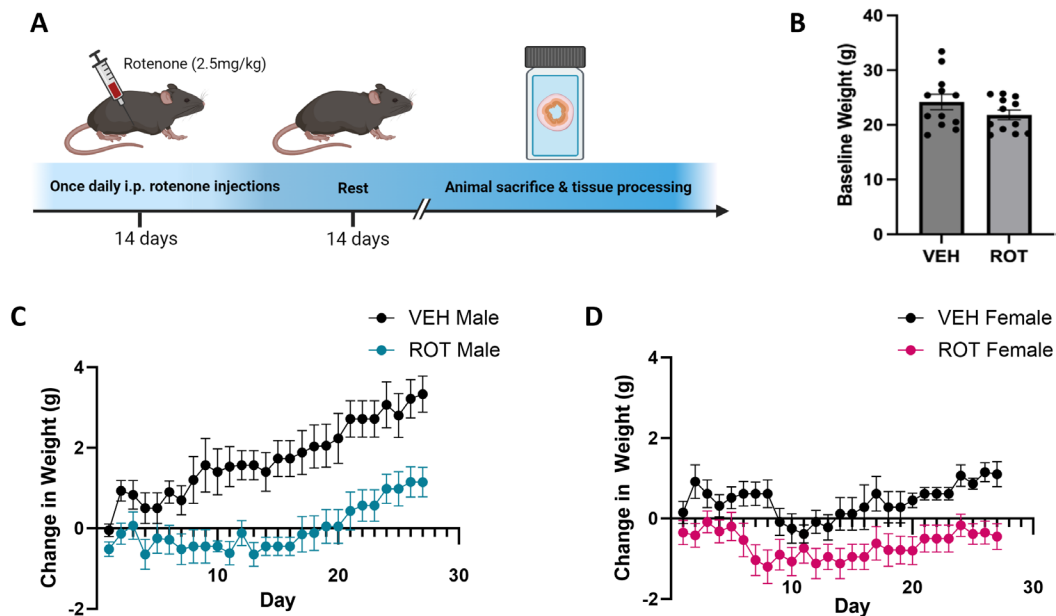


FIGURE 1 | Rotenone blunted weight gain in males and females. (A) Overview of the experimental timeline. (B) Baseline weights of male and female vehicle versus rotenone mice. (C) Average change in weight from baseline in males. (D) Average change in weight from baseline in females. VEH = vehicle, ROT = rotenone.

Following behavioral confirmation of impairment, intestinal sections were analyzed for myenteric neuronal changes using a peripheral neuronal marker, PGP 9.5. Total aSyn area increased in myenteric PGP 9.5⁺ neurons in males and females after 2 weeks of rotenone treatment, with an increase in immunoreactive (ir) aSyn of 203% in females ($1.5 \mu\text{m}^2 \pm 0.1$, $p < 0.0001$) and 50% in males ($1.3 \mu\text{m}^2 \pm 0.04$, $p < 0.05$) (Figure 1B) compared to vehicle-treated animals (females: 0.49 ± 0.10 , $p > 0.05$; males: 0.84 ± 0.11 , $p > 0.05$). A two-way ANOVA revealed a main effect of rotenone treatment ($F(1, 20) = 60.50$, $p < 0.0001$) and a significant interaction between sex and rotenone ($F(1, 20) = 10.55$, $p < 0.01$) indicating that rotenone's impact was reliably greater in females. This was due in part to vehicle-treated females starting with 58% ($0.49 \mu\text{m}^2 \pm 0.07$) less immunoreactive myenteric aSyn than vehicle-treated males ($p < 0.05$, Figure 2B). PGP 9.5-ir area was not different in males versus females after rotenone treatment (Interaction effect: $F(1, 17) = 0.177$, $p > 0.05$) (Figure 2C) indicating that increases in aSyn area were not a result of elevated ir-PGP 9.5⁺ cell area.

3.2 | Apical CGRP Fiber Quantities Elevated in Rotenone Treated Mice

CGRP fiber immunoreactivity was interrogated by crypt region (i.e., apical crypt vs. basal crypt) in separate two-way ANOVAs. In apical crypts, CGRP levels were greater in rotenone-treated animals ($F(1, 20) = 61.93$, $p < 0.0001$) (Figure 3A,C). This increase was 26% higher in females compared to males ($F(1, 20) = 9.74$, $p < 0.01$) (Figure 3C), driven by the rotenone-treated

groups, as there was no difference by sex in vehicle ($F(1, 20) = 2.89$, $p > 0.05$) and no sex by treatment interaction.

In basal crypt regions, the average percent area of CGRP-ir was low in males and females. There was, however, a main effect of sex ($F(1, 20) = 13.2$, $p < 0.05$) where male vehicle-treated animals had elevated basal CGRP-ir compared to vehicle-treated females (Figure 3D). The interaction of sex by treatment was not statistically significant, suggesting some reliability to the sex effect even though the sex difference between treated mice was small.

3.3 | Rotenone Treatment Increased aSyn in CGRP⁺ Myenteric Neurons and Apical Fibers

Immunoreactive aSyn was colocalized with CGRP⁺ myenteric neurons and apical mucosal fibers in a sex selective manner (Figure 4). Two-way ANOVA investigating aSyn in CGRP⁺ myenteric neurons revealed a main effect of rotenone treatment ($F(1, 20) = 58.37$, $p < 0.0001$). The percent area of aSyn in myenteric CGRP neurons (Figure 4A,B) was greater in males and females treated with rotenone (male $12\% \pm 1.2$; female $10\% \pm 0.6$) compared to vehicle (male $4.8\% \pm 0.7$, $p < 0.0001$; female $4.7\% \pm 0.7$, $p < 0.005$) (Figure 4A). Levels of aSyn in apical CGRP⁺ fibers (Figure 4C-E) were increased in rotenone treated mice ($F(1, 20) = 116.7$, $p < 0.0001$), of both sexes ($F(1, 20) = 6.21$, $p < 0.05$); however, females had a larger increase as demonstrated by a statistically significant interaction between sex and treatment ($F(1, 20) = 6.57$, $p < 0.05$). The percent area of aSyn in apical

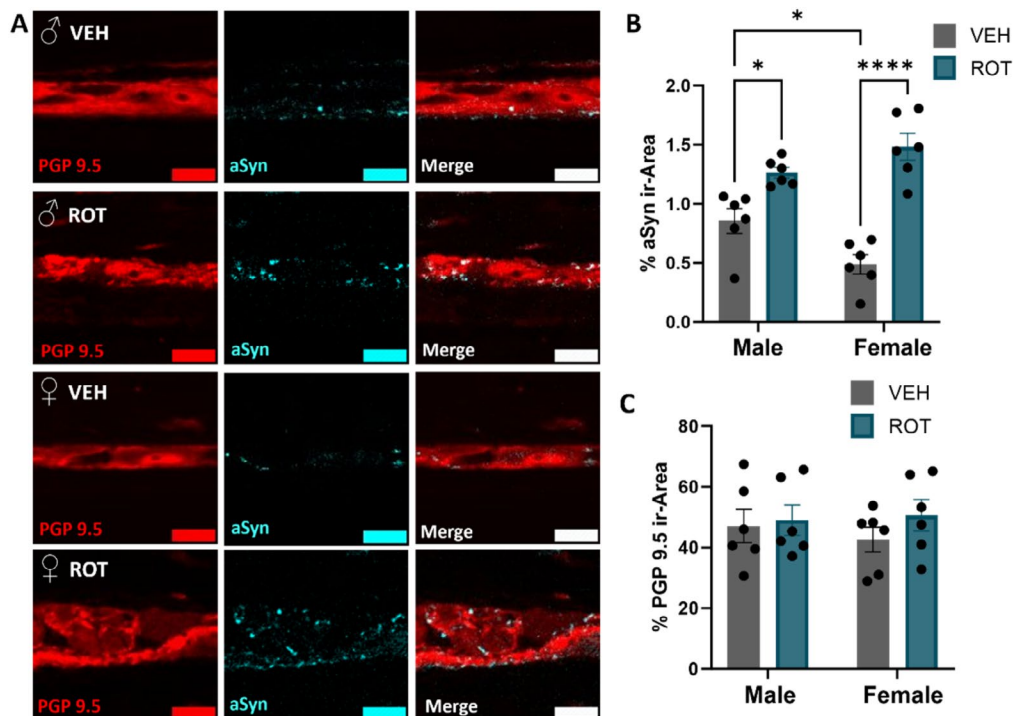


FIGURE 2 | Myenteric plexus aSyn was greater in colons from rotenone treated mice. (A) Compared to vehicle, both male and female proximal colon showed greater aSyn immunoreactivity in myenteric neurons with rotenone treatment. Females exhibited a larger increase in myenteric aSyn than males. (B) Quantification of aSyn immunoreactivity in the myenteric plexus. (C) Quantification of PGP 9.5 immunoreactivity in the myenteric plexus. Scale bars are $15 \mu\text{m}$, * $p < 0.05$, ** $p < 0.001$, **** $p < 0.0001$. VEH=vehicle, ROT=rotenone, aSyn=alpha synuclein, PGP9.5=protein gene product 9.5.

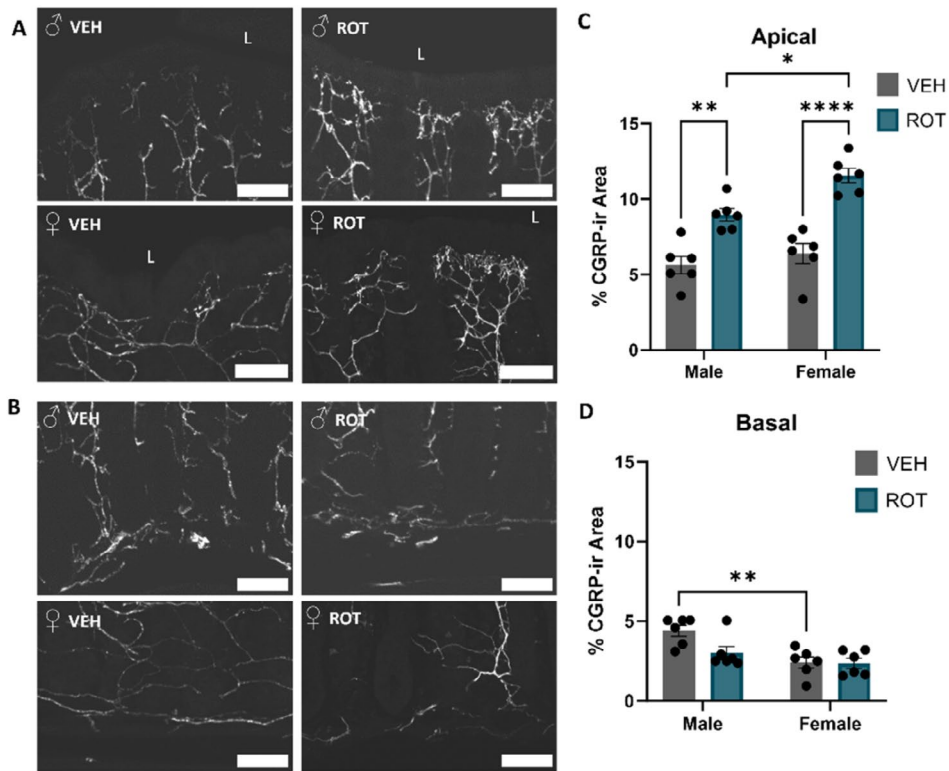


FIGURE 3 | Apical CGRP⁺ fiber quantities were elevated in colon crypts from rotenone treated mice. (A) Rotenone treatment increased the apical percent area of CGRP⁺ fibers in males and females. (B) Rotenone treatment did not alter basal percent area of CGRP⁺ fibers in males and females. (C) Quantification of average percent area of CGRP immunoreactivity in the apical crypt. (D) Quantification of average percent area of CGRP immunoreactivity in the basal crypt. Scale bars are 50 μ m, L = lumen, * p < 0.05, ** p < 0.001, **** p < 0.0001. VEH = vehicle, ROT = rotenone, CGRP = calcitonin gene related peptide.

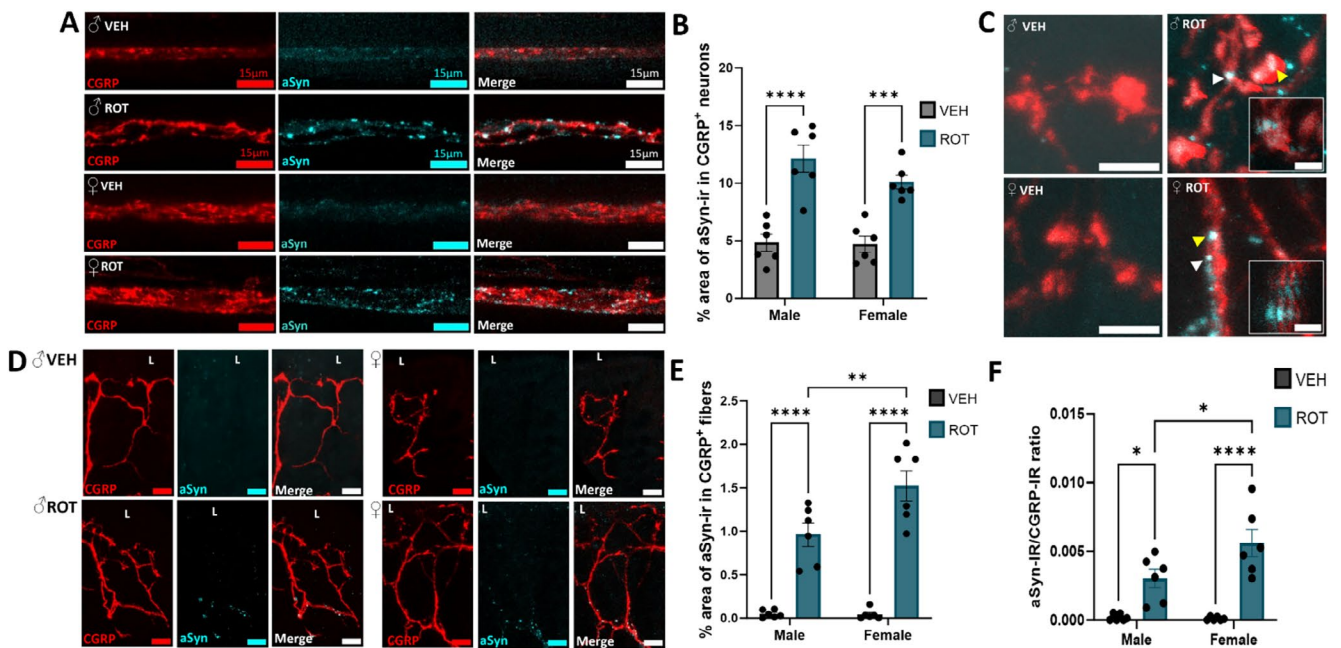


FIGURE 4 | Rotenone treatment increased aSyn in CGRP⁺ myenteric neurons and apical fibers. (A) Rotenone treatment increased the percent area of aSyn in myenteric CGRP neurons in males and females. (B) Rotenone treatment increased the percent area of aSyn in apical CGRP fibers in males and females. (C) High resolution images of aSyn-ir in apical CGRP varicosities. Arrows indicate areas of CGRP and aSyn colocalization, white arrows indicate region of inset. Insets are volume rendered cross-sections taken at a 60° angle. (D) Quantification of percent area of aSyn immunoreactivity in myenteric CGRP⁺ neurons. (E) Quantification of percent area of aSyn immunoreactivity in apical CGRP⁺ fibers. (F) Quantification of ratio of aSyn-IR in CGRP-ir fibers. Scale bars are 15 μ m for (A and D), for (C) scale bars are 5 and 2 μ m for insets. L = lumen, * p < 0.05, ** p < 0.001, **** p < 0.0001. VEH = vehicle, ROT = rotenone, CGRP = calcitonin gene related peptide, aSyn = alpha synuclein.

CGRP fibers was elevated in males (vehicle: $0.04\% \pm 0.02$, rotenone: $0.9\% \pm 0.1$, $p < 0.0001$) and females (vehicle: female $0.04\% \pm 0.02$, rotenone: $1.5\% \pm 0.2$, $p < 0.0001$) (Figure 4E). This increase was 67% higher in female animals compared to males ($p < 0.01$) (Figure 4E). To confirm this increase was not due to greater apical CGRP⁺-ir in rotenone treated animals, the ratio of aSyn-ir to apical CGRP was assessed. The ratio of aSyn-ir to apical CGRP-ir (Figure 4F) was increased in rotenone treated mice ($F(1, 20) = 47.94$, $p < 0.0001$), of both sexes ($F(1, 20) = 4.88$, $p = 0.05$); however, females had a larger increase as demonstrated by a statistically significant interaction between sex and treatment ($F(1, 20) = 4.879$, $p < 0.05$). The ratio of aSyn-IR to CGRP-ir was elevated in males (vehicle: 0.0002 ± 0.0001 , rotenone: 0.003 ± 0.007) and females (vehicle: $9.8e-05 \pm 5e-05$, rotenone: 0.006 ± 0.001) in rotenone treated mice compared to vehicle. This increase was 50% higher in female animals compared to males ($p < 0.05$).

3.4 | Goblet Cells Altered Morphologically After Rotenone Treatment

Mucopolysaccharides were fluorescently labeled with the lectin *Ulex europaeus* Agglutinin I (UEA1) and goblet cell size and number were analyzed by crypt region (i.e., apical vs. basal, Figure 5). A three-way ANOVA revealed a main effect of region ($F(1, 40) = 82.41$, $p < 0.001$) where apical goblet cell numbers were lower in animals treated with rotenone ($F(1, 40) = 12.92$, $p < 0.001$) regardless of sex ($F(1, 40) = 1.4$, $p > 0.05$) (Figure 5A–C). Males treated with rotenone had 53% fewer apical goblet cells (5.0 ± 0.1) (Figure 5B) compared to vehicle (10.0 ± 0.4 , $p < 0.0001$) (Figure 5A,C) and rotenone-treated females had 48% fewer cells (4.0 ± 0.2) compared to vehicle (8.0 ± 0.5 , $p < 0.0001$). Vehicle-treated males had 20% higher baseline goblet cell counts compared to females restricted to the apical region ($F(1, 40) = 13.07$, $p < 0.001$) (Figure 5C). There were 20% fewer basal goblet cells after rotenone treatment in males (10.0 ± 0.6) (Figure 5B') compared to vehicle (8.0 ± 0.3 ,

$p < 0.05$) (Figure 5A') a similar difference that did not reach statistical significance by post hoc testing in females (Figure 5C).

In contrast to fewer goblet cells after rotenone, those goblet cells that remained were larger. A three-way ANOVA investigating goblet cell size revealed a main effect of region ($F(1, 40) = 34.34$, $p < 0.001$) where goblet cell size was greater in rotenone-treated animals selectively in the apical crypt regions ($F(1, 40) = 12.36$, $p < 0.001$), with no main effect of sex ($F(1, 40) = 1.14$, $p > 0.05$) (Figure 5D). There was a main effect of treatment ($F(1, 40) = 40.95$, $p < 0.0001$) where apical goblet cell size was 79% greater in rotenone-treated males ($117.7 \mu\text{m}^2 \pm 6.1$) (Figure 5B) compared to vehicle-treated males ($65.9 \mu\text{m}^2 \pm 2.1$, $p < 0.001$) (Figure 5A) and 74% greater in rotenone-treated females ($135.3 \mu\text{m}^2 \pm 11.2$) compared to those treated with vehicle ($77.8 \mu\text{m}^2 \pm 6.7$, $p < 0.001$).

4 | Discussion

Females with PD exhibit faster disease progression and higher mortality rates than males [10]. Using a rotenone mouse model of PD, the results of the current study point towards sex-selective changes in enteric aSyn levels, alterations in CGRP distribution, and changes in goblet cell morphology, potentially influencing the more severe outcomes in females with PD. These findings contribute to our understanding of the link between intestinal homeostasis and aSyn aggregation in peripheral PD pathology and may provide insights for advancing early diagnostic strategies. Few studies of peripheral aSyn aggregation or PD pathological etiology include sex as a biological variable. Given that females with PD exhibit a higher mortality rate and report increased severity of GI symptoms [10, 11, 41], the present study provides an indication of potential sex-selective targets of a disease process.

Enteric aSyn levels are elevated in PD [42], and the pesticide rotenone increases aSyn in the central nervous system [37] and

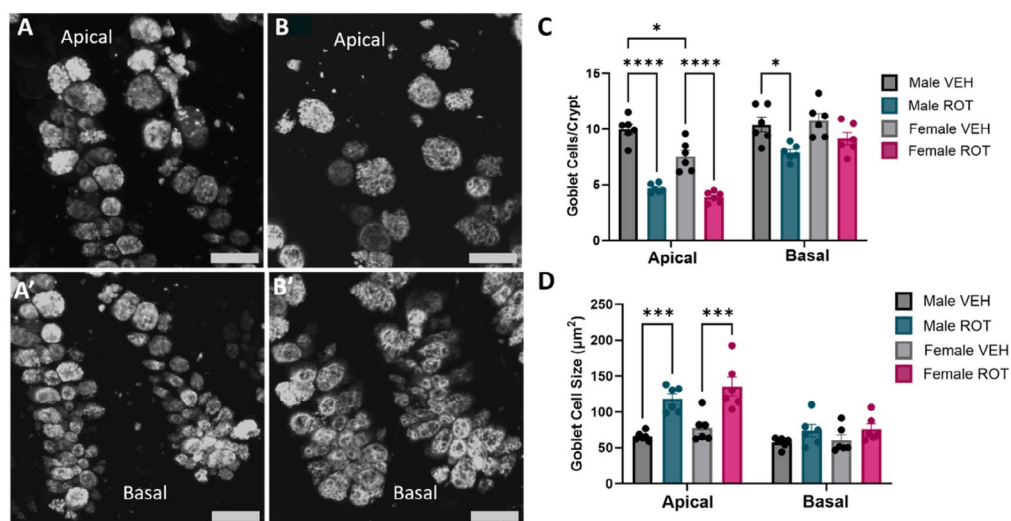


FIGURE 5 | UEA1⁺ goblet cells altered morphologically after rotenone treatment. (A) UEA1⁺ goblet cells at the apex and (A') base of the crypt in vehicle treated tissue have a smaller average immunoreactive area and are fewer in number than (B) UEA1⁺ goblet cells at the apex and (B') base of the crypt in rotenone-treated tissue. (C) Quantification of UEA1⁺ goblet cell number and (D) UEA1⁺ immunoreactive area. Scale bars 25 μm, representative images are male, * $p < 0.05$, *** $p < 0.001$ **** $p < 0.0001$. VEH = vehicle, ROT = rotenone, UEA1 = *Ulex europaeus* Agglutinin I.

the GI tract [43]. The present study demonstrated that intraperitoneal rotenone injections increased total aSyn in myenteric plexus neurons consistent with pathology found after oral rotenone administration [43]. There was a basal sex difference in myenteric aSyn levels, with males having higher quantities. When treated with rotenone, aSyn levels rose significantly in both sexes, but more so in females. This finding potentially implicates the female myenteric neuronal population as having an altered neurochemical phenotype at baseline, akin to the estrus cycle-dependent change in neuronal nitric oxide synthase (nNOS) neuron phenotype [44]. The lower baseline but subsequent post-rotenone compensation of aSyn levels in female CGRP neurons and fibers may influence GI motility and goblet cell secretory function. Together, these data provide a potential explanation for the more severe GI transit dysfunction in PD females. Further investigations of the impact of aSyn on GI motility and neuroepithelial signaling within the context of sex are clearly warranted [11, 14].

Neurons utilizing the neuropeptide CGRP for signaling may be critically involved in regulating intestinal motility and nociception [29, 45, 46]. Visceral pain is regulated by gut wall components, including the secretions from the microbiome adjacent to the colonic wall, and via enteric neuronal afferent CGRP signaling to the dorsal root ganglia [20, 33, 46]. Further, agonizing colonic CGRP receptors prior to colonic distention yields elevated visceral pain responses in conventionally colonized mice [20]. The increased CGRP⁺ apical fiber density observed in this study may contribute to elevated sensitivity to noxious stimuli from the lumen; however, receptor expression patterns for noxious ligands on apical CGRP⁺ fibers were not investigated in this study. The greater increase in apical CGRP in rotenone-treated females provides a focal point highlighting CGRP's potential involvement in the higher incidence of visceral pain observed in female PD patients. Studies examining CGRP receptor populations along with peptide release in these anatomically distinct enteric regions are needed to identify functional connections among the gut circuits identified here.

Alpha-synuclein aggregation can elicit morphological and firing pattern changes in neuronal populations [47]. Increased aSyn in CGRP⁺ enteric neurons may modulate downstream CGRP anatomical alterations and signaling patterns. CGRP production is upregulated in damaged nerves [23] and intraperitoneal injections of the CGRP antagonist BIBN 4096 BS decreased central aSyn expression in a mouse model of Alzheimer's disease [48]. Rotenone-treated males and females had increased aSyn in CGRP⁺ myenteric neurons and apical CGRP⁺ fibers, suggesting that aSyn levels may be related to alterations in gut CGRP neuronal immunoreactivity akin to those seen in PD patient-derived neuronal cultures [47, 49]. Female mice showed a greater increase in aSyn in apical CGRP⁺ fibers, a greater increase in immunoreactive CGRP in apical regions of colonic crypts, and lower baseline levels of myenteric aSyn compared to males, suggesting that females might be more susceptible to aSyn and CGRP localization within neuronal fibers following rotenone treatment.

Underlying causes of constipation, one of the earliest symptoms of PD [15, 16], are multifaceted, and treatment with anti-CGRP monoclonal antibodies decreases GI transit [29, 30]. Similarly,

animal studies with rotenone report decreased intestinal transit [8, 9]. In the present study, rotenone-treated mice exhibited increased area of CGRP immunoreactive fibers at the apical crypt. One explanation for the association between elevated gut mucosal CGRP and potential aSyn-driven constipation is through regulation of mucus production by goblet cells. In the current study, there were fewer goblet cells that were larger following rotenone treatment. The impact was stronger apically, coinciding with the greater CGRP fiber density after rotenone. Goblet cells originate from progenitor cells at the base of the crypts and mature as they migrate apically, where they acquire the ability to synthesize and secrete mucopolysaccharides [50]. Mature goblet cells are located in the upper third of crypts [51, 52] potentially making them more susceptible to morphological changes due to local environmental factors like dense CGRP-producing neuronal fibers. While acute stimulation of goblet cells serves as a protective mechanism to bolster the mucosal barrier in response to pathogens [53], chronic stimulation may lead to goblet cell mucus depletion. Impacts of aSyn-driven alterations to goblet cell mucus production and secretion remain unclear. The current results suggest a need to investigate goblet cell mucus production and mucosal thickness to determine if altered CGRP signaling after rotenone leads to mucosal barrier dysfunction.

5 | Conclusions

In conclusion, rotenone treatment reproduced PD clinical findings of increased aSyn in the myenteric plexus and extended these findings to show increases in apical CGRP immunoreactivity and altered goblet cell morphology in colonic crypts. Enteric aSyn may alter CGRP neuronal interactions with goblet cells that are critical for mucus production or secretion. These findings demonstrate a potential pathway for sex-selective neuronal-epithelial interaction between CGRP and goblet cells secondary to elevated enteric aSyn, identifying a potential contributor to GI dysfunction in PD. Since GI symptoms arise in a sex-specific manner, years before motor dysfunction, understanding mechanisms of enteric aSyn pathophysiology is crucial for identifying early diagnostic markers and novel therapeutic targets.

Author Contributions

Hayley N. Templeton: conceptualization, formal analysis, investigation, writing – original draft, visualization. **Alexis T. Ehrlich:** investigation, writing – review and editing. **Luke A. Schwerdtfeger:** conceptualization, formal analysis, writing – review and editing, supervision. **Julietta A. Sheng:** investigation. **Ronald B. Tjalkens:** methodology, resources. **Stuart A. Tobet:** conceptualization, supervision, project administration, funding acquisition, writing – review and editing.

Acknowledgments

We would like to thank Connie King (Department of Biomedical Sciences, Colorado State University, Fort Collins, CO, USA) for help with animal processing and Casey P McDermott (Department of Environmental and Radiological Health Sciences, Colorado State University, Fort Collins, CO, USA) for help with initial trial experiments and rotenone dosing protocol. We would also like to acknowledge the College of Veterinary Medicine and Biomedical Sciences Graduate Research Scholar Award for its partial support of these studies.

Conflicts of Interest

The authors declare no conflicts of interest.

Data Availability Statement

The data that support the findings of this study are available from the corresponding author upon reasonable request.

References

1. L. M. de Lau and M. M. Breteler, "Epidemiology of Parkinson's Disease," *Lancet Neurology* 5 (2006): 525–535, [https://doi.org/10.1016/S1474-4422\(06\)70471-9](https://doi.org/10.1016/S1474-4422(06)70471-9).
2. A. Fasano, N. P. Visanji, L. W. Liu, A. E. Lang, and R. F. Pfeiffer, "Gastrointestinal Dysfunction in Parkinson's Disease," *Lancet Neurology* 14 (2015): 625–639, [https://doi.org/10.1016/S1474-4422\(15\)00007-1](https://doi.org/10.1016/S1474-4422(15)00007-1).
3. R. A. Travagli, K. N. Browning, and M. Camilleri, "Parkinson Disease and the Gut: New Insights Into Pathogenesis and Clinical Relevance," *Nature Reviews. Gastroenterology & Hepatology* 17 (2020): 673–685, <https://doi.org/10.1038/s41575-020-0339-z>.
4. P. Calabresi, A. Mechelli, G. Natale, L. Volpicelli-Daley, G. di Lazzaro, and V. Ghiglieri, "Alpha-Synuclein in Parkinson's Disease and Other Synucleinopathies: From Overt Neurodegeneration Back to Early Synaptic Dysfunction," *Cell Death & Disease* 14 (2023): 176.
5. T. Warnecke, K. H. Schafer, I. Claus, K. del Tredici, and W. H. Jost, "Gastrointestinal Involvement in Parkinson's Disease: Pathophysiology, Diagnosis, and Management," *NPJ Parkinson's Disease* 8 (2022): 31.
6. J. R. Cannon, V. Tapias, H. M. Na, A. S. Honick, R. E. Drolet, and J. T. Greenamyre, "A Highly Reproducible Rotenone Model of Parkinson's Disease," *Neurobiology of Disease* 34 (2009): 279–290.
7. M. E. Johnson, A. Stringer, and L. Bobrovskaya, "Rotenone Induces Gastrointestinal Pathology and Microbiota Alterations in a Rat Model of Parkinson's Disease," *Neurotoxicology* 65 (2018): 174–185.
8. F. Pan-Montojo, M. Schwarz, C. Winkler, et al., "Environmental Toxins Trigger PD-Like Progression via Increased Alpha-Synuclein Release From Enteric Neurons in Mice," *Scientific Reports* 2 (2012): 898.
9. R. E. Drolet, J. R. Cannon, L. Montero, and J. T. Greenamyre, "Chronic Rotenone Exposure Reproduces Parkinson's Disease Gastrointestinal Neuropathology," *Neurobiology of Disease* 36 (2009): 96–102.
10. N. Dahodwala, Q. Pei, and P. Schmidt, "Sex Differences in the Clinical Progression of Parkinson's Disease," *Journal of Obstetric, Gynecologic, and Neonatal Nursing* 45 (2016): 749–756.
11. H. J. Chang, C. M. Shin, J. W. Cho, et al., "Sex Differences in Gastrointestinal Dysfunction Among Patients With Parkinson's Disease," *Neurological Sciences* 44 (2023): 2375–2384.
12. Q. Xiao-Ling, D. Yin-Zhen, L. Xue-Kui, et al., "Gender Was Associated With Depression but Not With Gastrointestinal Dysfunction in Patients With Parkinson's Disease," *Parkinson's Disease* 2021 (2021): 3118948.
13. M. Picillo, R. Palladino, R. Erro, et al., "The PRIAMO Study: Age- and Sex-Related Relationship Between Prodromal Constipation and Disease Phenotype in Early Parkinson's Disease," *Journal of Neurology* 268 (2021): 448–454.
14. A. A. Pilipovich, O. V. Vorob'eva, S. A. Makarov, N. N. Shindryaeva, and Y. D. Vorob'eva, "Gastrointestinal Dysfunction Impact on Life Quality in a Cohort of Russian Patients With Parkinson's Disease I-III H&Y Stage," *Parkinson's Disease* 2022 (2022): 1571801.
15. K. L. Adams-Carr, J. P. Bestwick, S. Shribman, A. Lees, A. Schrag, and A. J. Noyce, "Constipation Preceding Parkinson's Disease: A Systematic Review and Meta-Analysis," *Journal of Neurology, Neurosurgery, and Psychiatry* 87 (2016): 710–716.
16. M. G. Cersosimo, G. B. Raina, C. Pecci, et al., "Gastrointestinal Manifestations in Parkinson's Disease: Prevalence and Occurrence Before Motor Symptoms," *Journal of Neurology* 260 (2013): 1332–1338.
17. P. Perez-Pardo, H. B. Dodiya, L. M. Broersen, et al., "Gut-Brain and Brain-Gut Axis in Parkinson's Disease Models: Effects of a Uridine and Fish Oil Diet," *Nutritional Neuroscience* 21 (2018): 391–402.
18. S. L. Klein and K. L. Flanagan, "Sex Differences in Immune Responses," *Nature Reviews. Immunology* 16 (2016): 626–638.
19. L. A. Schwerdtfeger and S. A. Tobet, "Sex Differences in Anatomic Plasticity of Gut Neuronal-Mast Cell Interactions," *Physiological Reports* 9 (2021): e15066.
20. J. Pujo, G. de Palma, J. Lu, et al., "Gut Microbiota Modulates Visceral Sensitivity Through Calcitonin Gene-Related Peptide (CGRP) Production," *Gut Microbes* 15 (2023): 2188874.
21. N. M. Delvalle, C. Dharshika, W. Morales-Soto, D. E. Fried, L. Gaudette, and B. D. Gulbransen, "Communication Between Enteric Neurons, Glia, and Nociceptors Underlies the Effects of Tachykinins on Neuroinflammation," *Cellular and Molecular Gastroenterology and Hepatology* 6 (2018): 321–344.
22. R. Buckinx, L. van Nassauw, L. R. Avula, K. Alpaerts, D. Adriaensen, and J. P. Timmermans, "Transient Receptor Potential Vanilloid Type 1 Channel (TRPV1) Immunolocalization in the Murine Enteric Nervous System Is Affected by the Targeted C-Terminal Epitope of the Applied Antibody," *Journal of Histochemistry and Cytochemistry* 61 (2013): 421–432.
23. F. A. Russell, R. King, S. J. Smillie, X. Kodji, and S. D. Brain, "Calcitonin Gene-Related Peptide: Physiology and Pathophysiology," *Physiological Reviews* 94 (2014): 1099–1142.
24. P. K. Mulderry, M. A. Ghati, R. A. Spokes, et al., "Differential Expression of Alpha-CGRP and Beta-CGRP by Primary Sensory Neurons and Enteric Autonomic Neurons of the Rat," *Neuroscience* 25 (1988): 195–205.
25. K. Noguchi, E. Senba, Y. Morita, M. Sato, and M. Tohyama, "Alpha-CGRP and Beta-CGRP mRNAs Are Differentially Regulated in the Rat Spinal Cord and Dorsal Root Ganglion," *Brain Research. Molecular Brain Research* 7 (1990): 299–304.
26. K. Morarach, A. Mikhailova, V. Knoflach, et al., "Diversification of Molecularly Defined Myenteric Neuron Classes Revealed by Single-Cell RNA Sequencing," *Nature Neuroscience* 24 (2021): 34–46.
27. C. M. Wright, S. Schneider, K. M. Smith-Edwards, et al., "scRNA-Seq Reveals New Enteric Nervous System Roles for GDNF, NRTN, and TBX3," *Cellular and Molecular Gastroenterology and Hepatology* 11 (2021): 1548–1592, <https://doi.org/10.1016/j.jcmgh.2020.12.014>.
28. A. Nestor-Kalinowski, K. M. Smith-Edwards, K. Meerschaert, et al., "Unique Neural Circuit Connectivity of Mouse Proximal, Middle, and Distal Colon Defines Regional Colonic Motor Patterns," *Cellular and Molecular Gastroenterology and Hepatology* 13 (2022): 309–337, <https://doi.org/10.1016/j.jcmgh.2021.08.016>.
29. J. Ailani, E. A. Kaiser, P. G. Mathew, et al., "Role of Calcitonin Gene-Related Peptide on the Gastrointestinal Symptoms of Migraine-Clinical Considerations: A Narrative Review," *Neurology* 99 (2022): 841–853.
30. K. A. Haanes, L. Edvinsson, and A. Sams, "Understanding Side-Effects of Anti-CGRP and Anti-CGRP Receptor Antibodies," *Journal of Headache and Pain* 21 (2020): 26.
31. F. Fang, Y. Liu, Y. Xiong, et al., "Slowed Intestinal Transit Induced by Less Mucus in Intestinal Goblet Cell Piezo1-Deficient Mice Through Impaired Epithelial Homeostasis," *International Journal of Molecular Sciences* 24 (2023): 14377.
32. C. C. Gao, G. W. Li, T. T. Wang, et al., "Rhubarb Extract Relieves Constipation by Stimulating Mucus Production in the Colon and Altering the Intestinal Flora," *Biomedicine & Pharmacotherapy* 138 (2021): 111479.

33. D. Yang, A. Jacobson, K. A. Meerschaert, et al., “Nociceptor Neurons Direct Goblet Cells via a CGRP-RAMP1 Axis to Drive Mucus Production and Gut Barrier Protection,” *Cell* 185 (2022): 4190–4205 e4125, <https://doi.org/10.1016/j.cell.2022.09.024>.
34. J. R. Grider, “CGRP as a Transmitter in the Sensory Pathway Mediating Peristaltic Reflex,” *American Journal of Physiology* 266 (1994): G1139–G1145.
35. D. F. Sharrad, E. de Vries, and S. J. Brookes, “Selective Expression of Alpha-Synuclein-Immunoreactivity in Vesicular Acetylcholine Transporter-Immunoreactive Axons in the Guinea Pig Rectum and Human Colon,” *Journal of Comparative Neurology* 521 (2013): 657–676.
36. M. Swaminathan, C. Fung, D. I. Finkelstein, J. C. Bornstein, and J. P. P. Foong, “Alpha-Synuclein Regulates Development and Function of Cholinergic Enteric Neurons in the Mouse Colon,” *Neuroscience* 423 (2019): 76–85.
37. S. M. Rocha, “Rotenone Induces Regionally Distinct Alpha-Synuclein Protein Aggregation and Activation of Glia Prior to Loss of Dopaminergic Neurons in C57Bl/6 Mice,” *Neurobiology of Disease* 167 (2022): 105685, <https://doi.org/10.1016/j.nbd.2022.105685>.
38. B. Cao, “PDCD4 Triggers Alpha-Synuclein Accumulation and Motor Deficits via Co-Suppressing TFE3 and TFEB Translation in a Model of Parkinson’s Disease,” *npj Parkinson’s Disease* 10 Elsevier, (2024), <https://doi.org/10.1038/s41531-024-00760-9>.
39. M. Yu, H. Ye, R. B. de-Paula, et al., “Functional Screening of Lysosomal Storage Disorder Genes Identifies Modifiers of Alpha-Synuclein Neurotoxicity,” *PLoS Genetics* 19 (2023): e1010760, <https://doi.org/10.1371/journal.pgen.1010760>.
40. N. Uemura, N. P. Marotta, J. Ara, et al., “Alpha-Synuclein Aggregates Amplified From Patient-Derived Lewy Bodies Recapitulate Lewy Body Diseases in Mice,” *Nature Communications* 14 (2023): 6892.
41. S. Cerri, L. Mus, and F. Blandini, “Parkinson’s Disease in Women and Men: What’s the Difference?,” *Journal of Parkinson’s Disease* 9 (2019): 501–515.
42. A. Gold, Z. T. Turkalp, and D. G. Munoz, “Enteric Alpha-Synuclein Expression Is Increased in Parkinson’s Disease but Not Alzheimer’s Disease,” *Movement Disorders* 28 (2013): 237–240.
43. H. B. Dodiya, C. B. Forsyth, R. M. Voigt, et al., “Chronic Stress-Induced Gut Dysfunction Exacerbates Parkinson’s Disease Phenotype and Pathology in a Rotenone-Induced Mouse Model of Parkinson’s Disease,” *Neurobiology of Disease* 135 (2020): 104352.
44. G. K. Balasuriya, S. S. Nugapitiya, E. L. Hill-Yardin, and J. C. Bornstein, “Nitric Oxide Regulates Estrus Cycle Dependent Colonic Motility in Mice,” *Frontiers in Neuroscience* 15 (2021): 647555.
45. S. Iyengar, M. H. Ossipov, and K. W. Johnson, “The Role of Calcitonin Gene-Related Peptide in Peripheral and Central Pain Mechanisms Including Migraine,” *Pain* 158 (2017): 543–559.
46. M. S. Clifton, J. J. Hoy, J. Chang, et al., “Role of Calcitonin Receptor-Like Receptor in Colonic Motility and Inflammation,” *American Journal of Physiology. Gastrointestinal and Liver Physiology* 293 (2007): G36–G44.
47. P. Calabresi, G. di Lazzaro, G. Marino, F. Campanelli, and V. Ghiglieri, “Advances in Understanding the Function of Alpha-Synuclein: Implications for Parkinson’s Disease,” *Brain* 146 (2023): 3587–3597.
48. H. Na, Q. Gan, L. Mcparland, et al., “Characterization of the Effects of Calcitonin Gene-Related Peptide Receptor Antagonist for Alzheimer’s Disease,” *Neuropharmacology* 168 (2020): 108017.
49. M. Lin, P. M. Mackie, F. Shaerzadeh, et al., “In Parkinson’s Patient-Derived Dopamine Neurons, the Triplication of Alpha-Synuclein Locus Induces Distinctive Firing Pattern by Impeding D2 Receptor Autoinhibition,” *Acta Neuropathologica Communications* 9 (2021): 107.
50. S. Yang and M. Yu, “Role of Goblet Cells in Intestinal Barrier and Mucosal Immunity,” *Journal of Inflammation Research* 14 (2021): 3171–3183, <https://doi.org/10.2147/JIR.S318327>.
51. J. Merzel and M. L. Almeida, “Maturation of Goblet Cells of the Mouse Small Intestine as Shown by the Uptake of ³⁵S-Sodium Sulfate,” *Anatomical Record* 177 (1973): 519–524.
52. F. Noah and S. A. K. Shroyer, *Pediatric Gastrointestinal and Liver Disease*, vol. 31, ed. J. S. Hyams and R. Wyllie (Elsevier, 2011), 324–336.
53. R. D. Newberry and R. G. Lorenz, “Organizing a Mucosal Defense,” *Immunological Reviews* 206 (2005): 6–21.

Supporting Information

Additional supporting information can be found online in the Supporting Information section.